Proceedings of ASME Turbo Expo 2010: Power for Land, Sea, and Air
GT2010
June 14-18, 2010, Glasgow, UK

GT2010-23424

MEASUREMENTS OF EQUIVALENCE RATIO FLUCUTAITONS IN A LEAN PREMIXED GAS TURBINE COMBUSTOR USING AN IR ABSORPTION TECHNIQUE

Hyung Ju Lee[1], Kyu Tae Kim[2], Jong Guen Lee[3], Bryan D. Quay[4], and Domenic A. Santavicca[5]
Department of Mechanical and Nuclear Engineering
The Pennsylvania State University
University Park, PA 16802

ABSTRACT

An experimental study was conducted to estimate and confirm equivalence ratio fluctuations at the inlet of a lean premixed gas turbine combustor. Fuel injectors were placed at several locations in the mixing section of the combustor, in order to produce different instability characteristics due to the equivalence ratio fluctuations. An IR absorption technique was used to measure the equivalence ratio fluctuations at the inlet of the dump combustor. The measured IR signals were processed in two different ways and the results were compared to confirm the two calibrated equivalence ratio signals. The processed data showed that the two processing methods gave very similar results, and the phase of the measured equivalence ratio fluctuations at the combustor inlet by the IR absorption technique agreed well with that of equivalence ratio fluctuations predicted by time lags in the mixing section. It was, however, not possible to accurately predict the magnitude of the equivalence ratio fluctuations at the combustor inlet by the time lag analysis because the equivalence ratio fluctuations generataed at the fuel injection location is changed by mixing and diffusion as the fuel is convected through the combustor.

NOMENCLATURE

I	Intensity
L	Length or Location
MW	Molecular weight
P, p	Pressure
Q	Heat release rate
R	Gas constant
T	Period, Temperature
V	Mean velocity
c	Concentration
f	Frequency
l	Path length
m	Mass
$\Delta\theta$	Phase difference
Φ	Equivalence ratio
ε	Decadic molar absorption coefficient
τ	Convection time or Time lag

Subscript

a	Air
$dump$	Dump plane or Combustor inlet
f	Fuel
in	Inlet to the combustor
inj	Fuel injection
$mean$	Mean quantity
mix	Mixing section
st	Stoichiometric condition
u	Universal
Φ	Equivalence ratio

Superscript

'	Fluctuation quantity

[1] Graduate Research Assistant, Currently Senior Researcher, Agency for Defense Development, Republic of Korea
[2] Graduate Research Assistant, Currently Research Associate, Engineering Department, University of Cambridge, UK
[3] Senior Research Associate, Department of Mechanical and Nuclear Engineering
[4] Research Associate, Department of Mechanical and Nuclear Engineering
[5] Professor, Department of Mechanical and Nuclear Engineering

INTRODUCTION

Gas turbines for power generation are significant sources of combustion-generated greenhouse gases and NO_x emissions, and most gas turbine manufacturers use lean premixed combustion as the most successful strategy for reducing NO_x production. Reduced emissions, however, have been achieved at the expense of increased combustion instabilities. Therefore, the successful development of the next generation of ultra-low emissions lean premixed gas turbine (LPGT) combustors requires design tools based on stability models that can predict the relationships among combustor design, operating conditions, and combustion instability. Due to our limited understanding of the fundamentals of combustion instabilities, however, it is not currently feasible to design an LPGT combustor that is stable over its entire operating range, or to predict the operating conditions at which a given combustor will go unstable. As a result, extensive theoretical and experimental studies have been performed to identify the fundamental mechanisms associated with the initiation and growth of combustion instabilities [1-8].

Combustion instability mechanisms consist of various elementary processes that can be described as interactions between acoustic waves, flow perturbations and unsteady combustion, and some of them are specifically relevant to lean premixed gas turbine combustors; they are, for example, fuel feed line – acoustic coupling, flame area oscillations, flame-vortex interactions and equivalence ratio fluctuations [9]. Among various instability mechanisms, equivalence ratio fluctuations are observed most frequently along with flame-vortex interactions in practical lean premixed combustors [3, 5, 8, 10]. Equivalence ratio fluctuations are generated by fluctuations in the air and/or fuel flow rates at the fuel injector location, which are the result of acoustic pressure and velocity fluctuations [11]. When the resultant equivalence ratio fluctuations are convected to the combustor, they can act to amplify or damp the combustion instability, depending on whether they arrive at the flame front in-phase or out-of-phase with the existing heat release rate fluctuations [12]. Therefore, the equivalence ratio fluctuation at lean operating conditions can serve as a strong driving source of acoustic oscillations in a gas turbine combustor [11].

Gas turbine combustors typically consist of two sections: a mixing section and a combustion chamber. The mixing section is where the fuel is injected into the air flow and the fuel and air are mixed before they enter the combustor. If there are acoustic pressure and velocity fluctuations in the mixing section, both the air and fuel flow rates can fluctuate, which, in turn, results in equivalence ratio fluctuations [9]. In general, therefore, lean premixed combustors are susceptible to combustion instabilities driven by equivalence ratio fluctuations. There have been a number of theoretical and experimental studies on the effects of equivalence ratio fluctuations. To demonstrate the role of equivalence ratio fluctuations in the process of sustaining combustion instability, for example, Lee *et al*. [5, 13] performed an experimental study on a single-injector lean-premixed combustor. Based on simultaneous IR absorption and CH* chemiluminescence measurements of equivalence ratio fluctuations and heat release rate oscillations, they identified the effect of the equivalence ratio fluctuations by a time lag analysis. Few previous studies, however, have investigated systematically the fundamental mechanism of combustion instability driven by equivalence ratio fluctuations. Furthermore, even though some researchers have measured equivalence ratio fluctuations by IR absorption techniques and others have studied time lag analysis for equivalence ratio fluctuations, few studies have confirmed the estimated equivalence ratio fluctuations by IR measurement.

In this article, therefore, an experimental study is conducted to estimate and confirm equivalence ratio fluctuations at the inlet of a swirl-stabilized, lean-premixed, laboratory-scale gas turbine combustor. The primary objective is to identify the underlying mechanism of the generation of the equivalence ratio fluctuations in the mixing section, and to investigate the effectiveness of a time lag analysis. To achieve the goal, the combustor has been designed and manufactured so that the fuel injection location can be varied, which provides the capability of changing the time lag associated with the equivalence ratio fluctuations. Two-microphone measurement s are used to measure acoustic fields in the mixing section, and the equivalence ratio fluctuation at the inlet to the combustor is estimated using time lag analysis. In addition, the equivalence ratio fluctuation is measured by IR absorption technique. Specifically, to acquire the equivalence ratio fluctuations, the measured IR signals are processed in two different ways – by a calibration curve and a pressure correction from the theoretical formulation. After the two results are compared, the measured equivalence ratio fluctuations at the inlet to the combustor are compared with the time lag analysis estimates.

TIME LAG ANALYSIS

A time lag analysis can be applied to the equivalence ratio fluctuation instability mechanism. In this case, the fluctuation in the equivalence ratio is caused by fluctuations in the air and/or fuel flow rates at the location where the fuel is injected [2, 8, 11, 13]. The air flow rate fluctuation at the fuel injector location is determined by the acoustic velocity fluctuation in the mixing section, while fuel flow rate fluctuations are caused by pressure fluctuations at the injector location, which in turn cause the pressure drop across the injector to fluctuate if the fuel injector orifice is not choked. Depending on the impedance of the fuel injector, pressure fluctuations may also occur inside the injector, which can either enhance or dampen the fuel flow rate fluctuation. If the fuel injector orifice is choked, however, then the fuel flow rate is not affected by fluctuations in the mixing section pressure and the mass flow rate of fuel is constant. In this case, equivalence ratio fluctuations are still possible, due to fluctuations in the air flow rate at the injector location.

In any case, therefore, the acoustics in the mixing section plays an essential role in generating equivalence ratio fluctua-

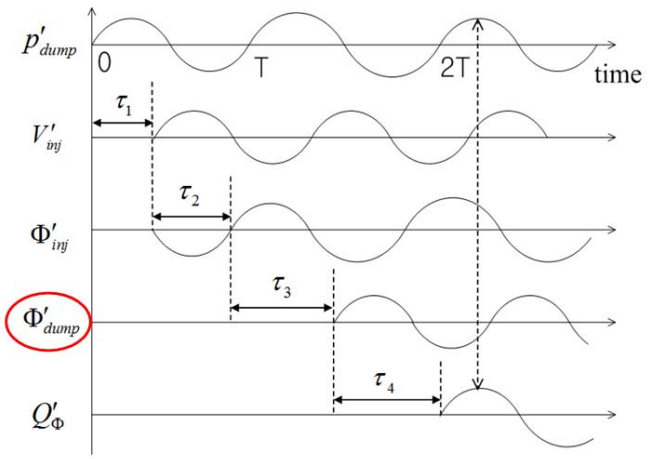

Figure 1. Illustration of the equivalence ratio fluctuation time lag analysis.

tions. When instability starts to grow, the acoustic field in the mixing section is driven at the dump plane by the pressure fluctuations in the combustor, and its response is dependent on the acoustic impedance of the mixing section. In other words, the pressure fluctuation at the dump plane will produce an upstream traveling wave in the mixing section, and it will reflect off the choked inlet when the wave reaches the upstream end of the mixing section, producing a downstream traveling wave. The resultant acoustics can be identified by two-microphone measurements [12].

Once the acoustic field in the mixing section is known, it is possible to perform an equivalence ratio fluctuation time lag analysis. The relationship between the pressure and velocity fluctuation in the mixing section and the resulting equivalence ratio fluctuation at the flame is illustrated in Fig. 1 [11], where the following assumptions have been made:

1) The fuel orifice is choked, so the fuel flow rate is constant.
2) The effect of the pressure fluctuation on the mass flow rate fluctuation of the air can be neglected because the magnitude of the acoustic velocity fluctuation in the mixing section is much greater than that of the acoustic pressure fluctuation.

Figure 1 shows time lags or phase relationships between the oscillating pressure, velocity, equivalence ratios, and rate of heat release when the combustor is unstable at one fundamental frequency. In case, therefore, that there are several main frequencies in practical situations, this analysis should be performed at each frequency separately. In the figure, τ_1 represents the time lag due to the phase difference between the combustor pressure and the velocity at the fuel injection location, τ_2 is the time lag between the oscillating velocity and the equivalence ratio fluctuation at the fuel injection location, τ_3 is the convection time of the equivalence ratio fluctuation from the fuel injector to the dump plane (i.e., the combustor inlet), and τ_4 represents the convection time of the equivalence ratio fluctuation from the dump plane to the flame. The figure shows that the time lags can be assessed as

$$\tau_1 = \frac{\Delta\theta_{p'_{dump}-V'_{inj}}}{360} T \quad (1)$$

$$\tau_2 = \frac{\Delta\theta_{V'_{inj}-\Phi'_{inj}}}{360} T \quad (2)$$

$$\tau_3 = \tau_{mix} = \frac{L_{inj}}{V_{in}} \quad (3)$$

where $\Delta\theta_{p'_{dump}-V'_{inj}}$ is the phase difference in degrees between the pressure at the dump plane and the velocity at the fuel injection location, $\Delta\theta_{V'_{inj}-\Phi'_{inj}}$ is the phase difference in degrees between the velocity and the equivalence ratio fluctuations at the fuel injection location (180° in the current case due to the choked fuel injector), τ_{mix} is the convection time of the equivalence ratio fluctuations from the fuel injector location to the dump plane, L_{inj} is the distance from the fuel injection location to the dump plane, and V_{in} is the mean inlet velocity. The time lag analysis shows that the equivalence ratio fluctuation at the dump plane marked by the red circle in Fig. 1 can be assessed once $\Delta\theta_{p'_{dump}-V'_{inj}}$ is known, by identifying the acoustic field in the mixing section from the two microphone method [12].

EXPERIMENTAL SETUP

Apparatus

A swirl-stabilized, lean-premixed, laboratory-scale combustor was manufactured to perform the experimental study. Figure 2(a) shows a photograph of the variable-fuel injector, variable-length combustor (PSU combustor). The combustor consists of a mixing section and a combustor section. The mixing section houses a movable fuel injector and a swirler; while the combustor section consists of an optically-accessible quartz section followed by a variable length steel section. A unique feature of this combustor is that both the fuel injection location and the combustion chamber length can be varied independently.

Figure 2(b) shows a schematic drawing of the mixing section, which includes a choked inlet, the fuel injector, the swirler and a bluff centerbody. There are also pressure taps for two-microphone measurement, a thermocouple tap for measuring the inlet temperature, and a window marked by the red circle in Fig. 2(b) for guiding an IR laser beam through the test section for the IR absorption measurement at a location 5 mm upstream of the dump plane. The mixing section is followed by the combustor section, which consists of a 115 mm diameter by 305 mm long quartz tube connected to a 76 mm diameter stainless steel tube. The overall length of the combustion chamber can be varied between 762 and 1,524 mm,

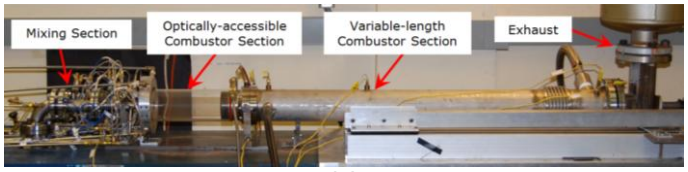

(a)

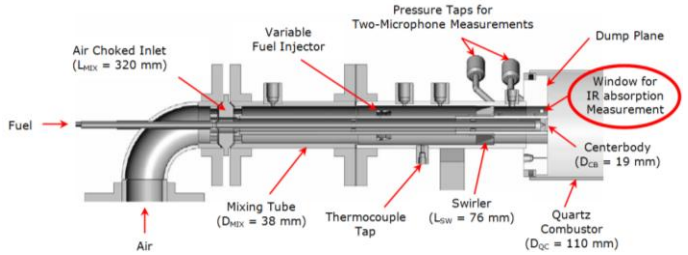

(b)

Figure 2. (a) Photograph of PSU combustor, and (b) schematic drawing of the mixing section.

which corresponds to a nominal factor of two variation in the acoustic frequency of the combustion chamber, by moving a stainless steel, water-cooled plug along the length of the stainless steel section of the combustion chamber. A more detailed description of the combustor configuration can be found in Ref. [12].

Test Conditions

Tests were conducted at a nominal combustor pressure of 1 atm over a range of operating conditions, as listed in Table 1. The air is heated to the inlet temperature by a regenerative heater which houses the variable length combustor and a 30 kW electric heater. Natural gas (96% methane) is used as fuel and injected either through the fuel injector into the mixing section or far upstream of the choked inlet. The latter case is referred to as "premixed (PM)" injection (see Table 1), which implies that there is no equivalence ratio fluctuation. The air and fuel flow rates are measured with linear mass flow meters (Teledyne-Hastings model HS-L100SF for the air and HS-10S for the fuel, respectively), which give an uncertainty in the inlet velocity of less than 2% and in the mean equivalence ratio of less than 3%.

MEASUREMENT TECHNIQUES

All measurements were made simultaneously at a sampling rate of 8192 Hz (per channel), and data were collected for 2 seconds, for a total of 16384 measurements (per channel). The corresponding time resolution and frequency resolution were 122 μs and 0.5 Hz, respectively.

Dynamic Pressure Measurements

To study the combustion instability due to equivalence ratio fluctuations, the combustion chamber dynamic pressure and the acoustic pressure in the mixing section were measured at the

Table 1. Operating conditions for the experiments

Parameters	Values
Inlet Temperature, T_{in}	473 K (200 °C)
Inlet Velocity, V_{in}	100 m/s
Equivalence Ratio, Φ	0.65
Fuel Injection Location, L_{inj}	152, 178, 203, 229, 254, 279, 305 mm (6, 7, 8, 9, 10, 11, 12") Premixed (PM)
Combustor Length, L_c	1,041 mm (41 inch)

operating conditions in Table 1. The dynamic pressure in the combustor is the most basic measurement in studies of unstable combustion. A water-cooled high-frequency response piezo-electric pressure transducer (PCB model 112A04) is flush mounted in the dump plane to measure the pressure oscillations in the combustor. The transducer output is amplified and converted to a voltage signal by an in-line charge amplifier. The frequency spectrum of the combustor pressure signal is used to determine the instability frequency and strength.

The acoustic pressure and velocity fluctuations in the mixing section are acquired by the two-microphone measurement [14, 15]. Two piezoelectric pressure transducers were mounted in the mixing section at locations 13mm and 51mm upstream of the dump plane, as shown in Figure 2(b). Using the two-microphone method, the pressure measurements are used to calculate the acoustic pressure and velocity fluctuations along the length of the mixing section. The velocity fluctuation determined by the two microphone method was verified by hot film anemometry measurements at the mid-point of the two microphone locations under cold flow conditions [16]. Similarly, the pressure fluctuation in the mixing section determined by the two microphone method was validated by pressure measurements made at seven locations along the length of the mixing section [12]. The acoustic pressure and velocity in the mixing section as resolved by the two-microphone method is used for the time lag analysis (see Fig. 1).

Measurement of the Equivalence Ratio Fluctuations

The technique for measuring equivalence ratio fluctuations is based on the absorption of the He-Ne laser at 3.39 μm by methane. The use of IR absorption for the measurement of the hydrocarbon concentrations in combustion systems has been well documented [5, 13, 17, 18]. A schematic of the IR absorption measurement is shown in Figure 3. The 3.39 μm output from a He-Ne laser is split into two beams by a beam splitter. The reflected beam is directed to a thermoelectrically cooled indium arsenide (InAs) detector to measure laser power variations. The transmitted beam is collimated into a 3 mm dia-

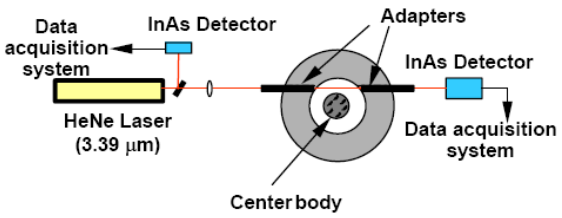

Figure 3. Schematic of the IR absorption measurement technique from Ref. [5].

meter beam by a lens, and passes through the test section via two cylindrical adapters with sapphire windows mounted in the dump body of the combustor. The adapters provide the optical access required for transmitting the laser beam across the entire test section. After it passes through the test cell, the beam is guided into the second thermoelectrically cooled InAs detector.

Theoretical background for IR absorption measurements is based on Beer-Lambert's law, which is known as

$$\log(I/I_0) = -\varepsilon c_f l \tag{4}$$

where I is the intensity of transmitted light through the absorbing species, I_0 is the intensity of incident monochromatic light, ε is the decadic molar absorption coefficient, c_f is the concentration of absorbing species, and l is the absorption path length. It is assumed in Eq. (4) that the concentration of the absorbing species is uniform through the beam path. Note, however, that the absorption of the laser beam, I/I_0 in Eq. (4), varies with the actual fuel distribution over the beam path, since absorption measurement is a line-of-sight integration. The law states explicitly the relationship between the concentration of a fuel in a mixture and the measured IR absorption signal. The fuel concentration is determined by modifying Eq. (4) as

$$c_f = -\frac{\log(I/I_0)}{\varepsilon l} \tag{5}$$

To obtain equivalence ratio fluctuations from the measured IR absorption signals, one needs to derive an equation that describes the relationship between the two. From the definition of equivalence ratio,

$$\Phi \equiv \frac{m_f/m_a}{(m_f/m_a)_{st}} = C_1 \frac{m_f}{m_a} = C_1 \frac{c_f}{c_a} \cdot \frac{MW_f}{MW_a} = C_2 \frac{c_f}{c_a} \tag{6}$$

where $C_2 = C_1 \frac{MW_f}{MW_a} = \frac{MW_f/MW_a}{(m_f/m_a)_{st}} = 9.518$ for a CH_4 and air mixture. Because $c = c_a + c_f$, substituting $c_a = c - c_f$ in Eq. (6) and rearranging yields,

$$c_f = \frac{c\Phi}{\Phi + C_2} \tag{7}$$

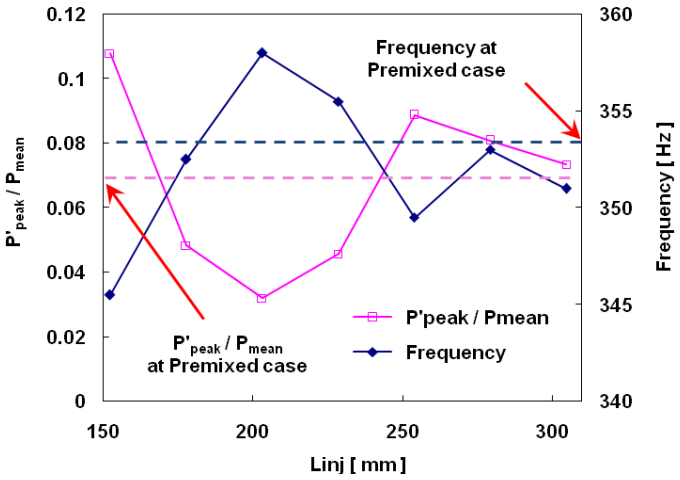

Figure 4. Instability strength and fundamental frequency for varying fuel injection locations at the operating condition; T_{in} = 473 K, V_{in} = 100 m/s, Φ = 0.65, and L_c = 1041 mm.

Substituting Eq. (7) into Eq. (5),

$$\log(I/I_0) = -\varepsilon l \frac{c\Phi}{\Phi + C_2} \tag{8}$$

Substituting the ideal gas law, $c = \frac{P}{R_u T}$, into Eq. (8) and rearranging it for Φ yields,

$$\Phi = -\frac{C_2 \log(I/I_0)}{\frac{\varepsilon P l}{R_u T} + \log(I/I_0)} \tag{9}$$

The equivalence ratio is thus directly related to the IR absorption signal. Once the time varying IR signal is measured, therefore, the time varying equivalence ratio is calculated by Eq. (9).

RESULTS AND DISCUSSION

Instability Characteristics for Varying Fuel Injection Locations

The combustor was found to be unstable at the combustor length of 1041 mm at the operating conditions listed in Table 1. Figure 4 shows the instability characteristics with respect to fuel injection location for this operating condition. The instability strength is represented by P'_{peak}/P_{mean}, which is a normalized pressure fluctuation magnitude at the fundamental instability frequency for each fuel injection location. This shows that P'_{peak}/P_{mean} varies significantly as the fuel injection location moves; the strength reaches up to 10.8% of the mean pressure at L_{inj} = 152 mm while it drops to 3.2% at L_{inj} = 203 mm. Note,

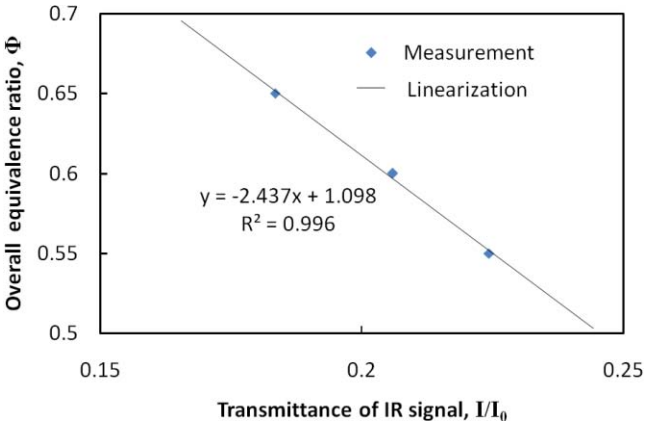

Figure 5. Normalized transmittance for premixed mixture at the operating condition listed in Table 1 without combustion.

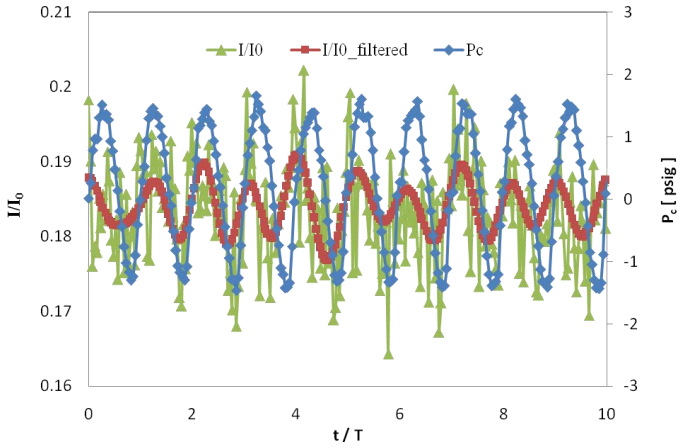

Figure 6. Measured IR signal for the premixed case at T_{in} = 473 K, V_{in} = 100 m/s, Φ = 0.65.

however, that the fundamental instability frequency does not change that much; it only moves from 345 to 357 Hz. The figure also shows the instability strength and frequency for the premixed case for comparison purposes. The strength is 6.9% of the mean pressure and the fundamental frequency is approximately 353 Hz for the premixed case. The figure shows, thus, that the instability in the partially premixed cases is amplified or damped as compared to that of the premixed case, due to the effect of changes in equivalence ratio fluctuations, as the fuel injection location is varied.

Equivalence Ratio Fluctuations from Calibration Curve

One way to acquire equivalence ratio fluctuations from the transmittance of the IR beam is by using a calibration curve [13]. From a separate experiment at the operating condition described in Table 1 in the same combustor without combustion, the calibration curve which describes a relationship between the normalized transmittance and the overall equivalence ratio is obtained, as shown in Figure 5. A time varying transmittance of the IR laser beam can thus be converted into the corresponding equivalence ratio fluctuation, assuming that the spatial equivalence ratio distribution across the beam path is unchanged during unstable combustion, even though the temporal equivalence ratio changes. The equivalence ratio fluctuations determined using the calibration curve at two fuel injection locations are shown in Fig. 8. They will be compared with results obtained using the other technique in the next section.

Equivalence Ratio Fluctuations from Theory, with Pressure-correction

As shown in Eq. (9), the equivalence ratio fluctuations, Φ(t), for partially premixed cases can be obtained from the theoretical formulation. In using Eq. (9), however, the decadic molar absorption coefficient, ε, is needed, in addition to the normalized measured intensity of IR signals, I/I_0. A previous study in Ref. [13] shows that ε is a function of the operating temperature and pressure. In this study, the temperature at the dump plane is fixed as 473K, while the pressure at the location varies when the combustor is unstable. Therefore, ε is not a constant, even though the operating condition is fixed, because the pressure at the measuring point fluctuates when the instability is present. To simply account for the effect of pressure on ε, one defines a factor A as

$$A \equiv \frac{\varepsilon l}{R_u T} \tag{10}$$

Note that A is a function of pressure and temperature because ε is a function of the two parameters. Using Eq. (10), Eq. (9) becomes

$$\Phi = -\frac{C_2 \log(I/I_0)}{P \cdot A + \log(I/I_0)} \tag{11}$$

In the current study, instead of measuring ε to get A using Eq. (10), the correlation of A with respect to pressure from the measured IR signal of the premixed case can be obtained by modifying Eq. (11), using the fact that the equivalence ratio does not fluctuate in that case., i.e.

$$A = -\frac{\log(I/I_0)}{P}\left(1 + \frac{C_2}{\Phi}\right) \tag{12}$$

where Φ is constant for the premixed case. Note also that A is a function of pressure because the inlet temperature is fixed as T_{in} = 473K. In Figure 6, the raw and filtered intensity of the normalized transmitted IR signals are presented along with the combustor pressure. Note that the filtered IR signal is acquired by filtering the raw signal digitally between 150 and 450 Hz during the post-processing, and it is included in the figure to in-

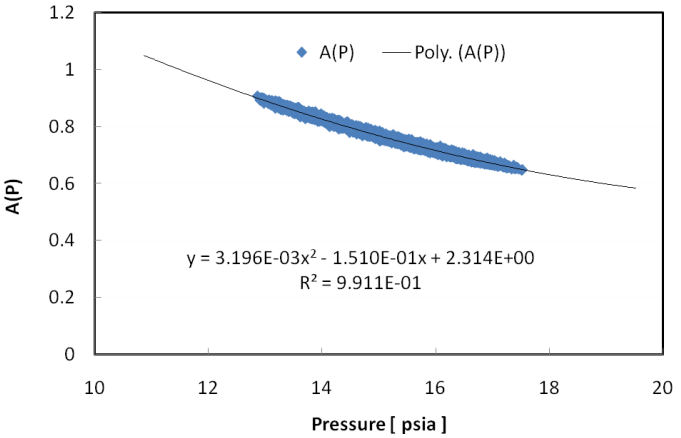

Figure 7. Correlation of A with respect to pressure obtained from the filtered signal of the premixed case.

vestigate the measured IR signal near the fundamental frequency component clearly. The figure shows that the IR signals oscillate with time in the premixed condition and are strongly coupled with the combustor pressure. From the measured data for the premixed condition, the relationship between A and pressure is given in Figure 7. Note that the band-pass filtered IR signal was used in Fig. 7 to get a better correlation between A and pressure. Once the correlation of A(P) is achieved, the equivalence ratio fluctuations are calculated for partially premixed cases using Eq. (11); they are the pressure-corrected equivalence ratio signals.

Figure 8 shows equivalence ratio fluctuations acquired by the two different methods; one is from the calibration curve in Fig. 5 and the other is from the pressure correction technique. Note that

$$\frac{\Phi'}{\Phi_{mean}} = \frac{\Phi - \Phi_{mean}}{\Phi_{mean}} \qquad (13)$$

so the quantity fluctuates around zero, and the signals shown in the figure were digitally filtered between 150 and 450 Hz for clearer comparison. The figure shows that there are small differences between the two results. Specifically, the difference is up to 3.7% at the fuel injection location of 152 mm, but the phases of the two equivalence ratio fluctuation signals are identical for both fuel injection locations. Even though the degree of premixedness for partially premixed cases will be a little different from that for the premixed case, the equivalence ratio fluctuations for the two partially premixed cases which were obtained from the calibration curve of the premixed case show quite good agreement with the equivalence ratio fluctuations acquired by the pressure correction technique. This implies two things; the effect of pressure on the resultant equivalence ratio fluctuations is small, and the degree of premixedness in this combustor is quite uniform for partially premixed cases, as compared with the premixed condition. Fig. 8(b) shows that the magnitude of the equivalence ratio fluctuation at L_{inj} = 203 mm is very small as compared with that of L_{inj} = 152 mm because the instability strength represented by P'_{peak}/P_{mean} of L_{inj} = 203 mm is 0.032, which is much smaller than that of L_{inj} = 152 mm, 0.108, as seen in Fig. 4. Quantitatively, looking at the magnitude of the measured IR intensity represented by I/I_0 at the fundamental instability frequency, that of L_{inj} = 203 mm case is 0.020 while that of L_{inj} = 152 mm is 0.182. It also shows that the signal at L_{inj} = 203 mm does not keep its magnitude with time, while the magnitude of the signal at L_{inj} = 152 mm remains almost constant. The reason for this phenomenon will be discussed below.

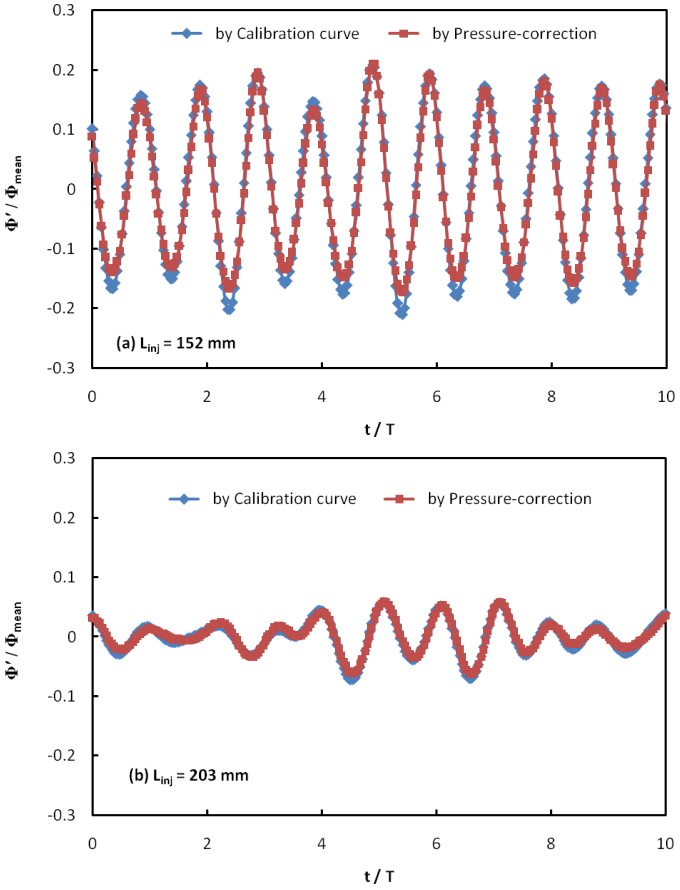

Figure 8. Comparison of the equivalence ratio fluctuations acquired by the calibration curve and by the pressure-correction; (a) L_{inj} = 152 mm, and (b) L_{inj} = 203 mm.

Comparison of Measured and Estimated Equivalence Ratio Fluctuations

Comparison of the equivalence ratio fluctuations at the dump plane measured by IR absorption and estimated by the time lag at L_{inj} = 152 and 203 mm is shown in Figure 9. Fig. 9(a) shows Φ'/Φ_{mean} from the measured raw IR signal, Φ'/Φ_{mean} from the IR signal filtered digitally between 150 and 450 Hz, and Φ'/Φ_{mean} estimated by the time lag analysis. The raw and the filtered Φ'/Φ_{mean} obtained from the measurement differ only sli-

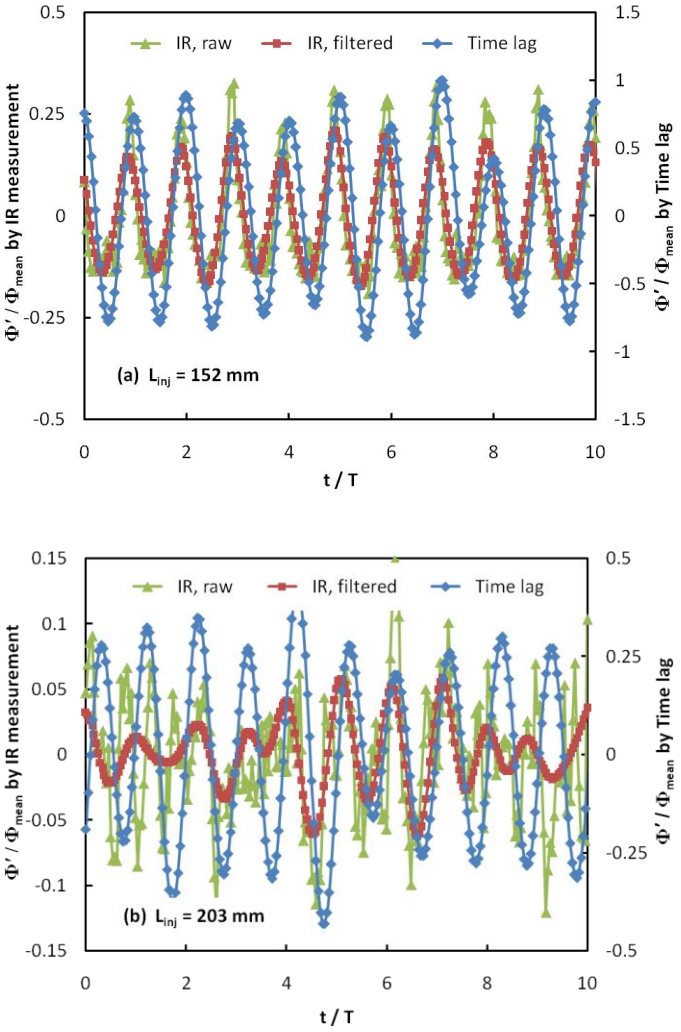

Figure 9. Comparison of the equivalence ratio fluctuations at the dump plane measured by the IR measurement and estimated by the time lag analysis.

ghtly, which means that the magnitude at the fundamental frequency is very strong compared with those of high and low frequency components. The phases of the measured and the estimated Φ'/Φ_{mean} are very close, which supports the estimation of the phases of equivalence ratio fluctuation at the dump plane by the time lag analysis. The magnitudes, however, of the measured and the estimated Φ'/Φ_{mean} are quite different; the amplitude of the measured Φ'/Φ_{mean} is approximately 25% of the estimated amplitude. From the fact that the time lag analysis considers only the phase relationships between the signals at each location, as shown in Fig. 1, the magnitude of Φ'/Φ_{mean} estimated from the time lag has little meaning. In other words, the estimation is based on the velocity fluctuation at the fuel injection location. The effects of mixing and diffusion on the generated equivalence ratio fluctuations during the convection from the fuel injector to the dump plane were not considered in the analysis. Future work should include a more detailed, systematic investigation of the effects of mixing and diffusion on equivalence ratio fluctuations during convection.

Figure 9(b) shows similar information for the case of L_{inj} = 203 mm. As in Fig. 9(a), the magnitude of the measured and the estimated Φ'/Φ_{mean} vary considerably; the magnitude of the measured signal is less than 20% of the magnitude of the estimated one. In addition, as described in the explanation of Fig. 8(b), the magnitude of the measured IR signal is very small, because the instability is the weakest at this fuel injection location. Unlike Fig. 9(a), however, there is quite a big difference between the raw and the filtered signals in this case, because the amplitude of the fundamental frequency component of the fluctuation is very small and the magnitude of the high and low frequency noise components are comparable to that of the main frequency component. In other words, if there was only the raw signal in Fig. 9(b), it would be hard to see clearly whether the measured equivalence ratio fluctuation is close to the estimated one or not because the intensity of the signal at the fundamental frequency is very low. Filtering out the signals unrelated to the main frequency component shows that the magnitude of the measured equivalence ratio fluctuation varied with time, and the measured IR signal coincided with the estimated one when the magnitude of the measured IR signal was strong, and vice versa. This observation suggests two important points: first, the generated equivalence ratio fluctuation at L_{inj} = 203 mm did not keep its harmonically oscillating feature at the dump plane because its intensity was originally weak (from the fact that the instability strength was the weakest at this fuel injection location) and, therefore, the effect of mixing and diffusion during its convection to the dump plane spoiled its original harmonic waveform. Second, even though the waveform of the equivalence ratio fluctuation at L_{inj} = 203 mm lost its harmonic nature for most of the time, it still showed us that the equivalence ratio fluctuation estimated by the time lag analysis coincided with the measured one when its intensity remained relatively strong, for $5 < t/T < 8$. This supports the validity of the time lag analysis. Though the results for only two fuel injection locations are shown in this paper, results for six other fuel injection locations also confirm that the estimation of equivalence ratio fluctuations at the dump plane by the time lag analysis was accurate within a phase difference of ±70 degrees, as compared with the measured data (see Table 2).

Table 2 shows a comparison of the phase differences between the measured and the estimated equivalence ratio fluctuations at the dump plane at four fuel injection locations: L_{inj} = 152, 203, 254, and 305 mm. All of the phase differences represented by $\Delta\theta_{IR\ -\ time\ lag}$ are less than 70°, except the case when the IR signal is the weakest (at L_{inj} = 203 mm). This means that the time lag model estimates the phase of the equivalence ratio fluctuations at the dump plane reasonably well, with errors of less than 70° in most cases. Seeing that the phase difference of Figure 9(a) is 41°, as shown in Table 2, one can deduce that estimation with errors less than 70° is quite good. The only case when the phase difference is bigger than

Table 2. Comparison of the phase differences between the measured and the estimated equivalence ratio fluctuations at the dump plane

L_{inj} [mm]	152	203	254	305
P' / P_{mean}	0.108	0.032	0.089	0.073
I' / I_{mean}	0.182	0.020	0.038	0.036
$\Delta\theta_{IR - time\ lag}$	41°	119°	-48°	-67°
Coherence	0.999	0.907	0.997	0.997

90° is when the fuel injector is located at 203 mm. The coherence at the fundamental instability frequency in the L_{inj} = 203 mm case is calculated as 0.907. Considering that the signals were acquired for only 2 seconds and the coherences for other fuel injection locations in Table 2 are above 0.990, the coherence for the L_{inj} = 203 mm case is relatively low. Recalling that the coherence function has rather slow convergence to its final value [19], more sampling time will be required to reach the final coherence value. In any case, the relatively low coherence means that the phase of the measured equivalence ratio fluctuation signal is not consistent in the L_{inj} = 203 mm case, as observed visually in Fig. 9(b). It is believed that both the magnitude and the phase of the IR signal vary with time in this case, partly because the originally weak signal was almost diffused out from time to time during the convection from the fuel injection location to the dump plane.

CONCLUSIONS

An experimental study was conducted to estimate and confirm equivalence ratio fluctuations at the inlet of a swirl-stabilized, lean-premixed, laboratory-scale gas turbine combustor. The primary objective was to identify the underlying mechanism of the generation of the equivalence ratio fluctuations in the mixing section of the combustor, and to investigate the effectiveness of a time lag analysis. To achieve the goal, the combustor has been designed and manufactured so that the fuel injection location can be varied, which provides the capability of changing the time lag associated with the equivalence ratio fluctuations. Based on measured acoustic fields in the mixing section of the combustor, the equivalence ratio fluctuation at the inlet to the combustor was estimated using the time lag analysis. In addition, the equivalence ratio fluctuation was measured by IR absorption. The measured IR signals were processed in two different ways to obtain the equivalence ratio fluctuations – using a calibration curve and using a pressure correction from the theoretical formulation. Results showed that the equivalence ratio fluctuations at the inlet as determined by the two techniques agreed quite well, within 3.7%. Then, the measured equivalence ratio fluctuations at the dump plane were compared with those estimated by the time lag analysis, and the time lag analysis in assessing the phase of the equivalence ratio fluctuations at the dump plane was found to be effective. The mechanism of the generation of the equivalence ratio fluctuations at the dump plane as represented by the time lag analysis is thus confirmed to be valid. The amplitudes of the measured and estimated equivalence ratio fluctuations are quite different, because of the effects of mixing and diffusion on the equivalence ratio fluctuations during convection from the fuel injector location to the dump plane. An investigation, therefore, on the systematic relationship between the amplitudes of the measured and estimated equivalence ratio fluctuations is left as a future work. In addition, the reason why a relatively modest displacement of the fuel injector causes such a dramatic increase in equivalence ratio fluctuations, in turn, the instability strength when the fuel injector was shifted from L_{inj} = 203 mm to 152 mm should be studied in the next stage.

ACKNOWLEDGMENTS

The authors are grateful for financial support provided by the National Science Foundation under NSF Award #0625970.

REFERENCES

[1] Fleifil, M., Annaswamy, A.M., Ghoniem, Z.A., and Ghoniem, A.F., 1996, "Response of a Laminar Premixed Flame to Flow Oscillations: A Kinematic Model and Thermodynamic Instability Results," *Combustion and Flame*, Vol. 106, No. 4, pp. 487-510

[2] Straub, D.L., and Richards, G.A., 1998, "Effect of Fuel Nozzle Configuration on Premix Combustion Dynamics," *ASME Paper* 98-GT-492

[3] Torres, H., Lieuwen, T.C., Johnson, C., Daniel B.R., and Zinn, B.T., 1999, "Experimental Investigation of Combustion Instabilities in a Gas Turbine Combustor Simulator," *AIAA Paper* 99-0712

[4] Cohen, J., and Anderson, T., 1999, "Experimental Investigation of Near-Blowout Instabilities in a Lean Premixed Combustor," *AIAA Paper* 1996-0819

[5] Lee, J.G., Kim, K., and Santavicca, D.A., 2002, "A Study of the Role of Equivalence Ratio Fluctuations during Unstable Combustion in a Lean Premixed Combustor," *AIAA Paper* 2002-4015

[6] Huang, Y., Sung, H.-G., Hsieh, S.-Y., and Yang, V., 2003, "Large-Eddy Simulation of Combustion Dynamics of Lean-Premixed Swirl-Stabilized Combustor," *Journal of Propulsion and Power*, Vol. 19, No. 5, pp. 782-794

[7] Dowling, A.P., and Stow, S.R., 2003, "Acoustic Analysis of Gas Turbine Combustors," *Journal of Propulsion and Power*, Vol. 19, No. 5, pp. 751-764

[8] Auer, M.P., Hirsch, C., and Sattelmayer, T., 2005, "Influence of the Interaction of Equivalence Ratio and Mass Flow Fluctuation on Flame Dynamics," *Proceedings of ASME Turbo Expo 2005*, GT2005-68373

[9] Zinn, B.T., and Lieuwen, T.C., 2005, "Combustion Instabilities: Basic Concepts," Ch. 1 in Lieuwen, T.C., and Yang. V. (Ed.), *Combustion instabilities in gas turbine engines: Operational experience, fundamental mechanisms, and Modeling*, Progress in Aeronautics and Aeronautics Series, Vol. 210, AIAA, Chapter 1

[10] Richards, G.A., Janus, M., and Robey, E.H., 1999, "Control of Flame Oscillations with Equivalence Ratio Modulation," *Journal of Propulsion and Power*, Vol. 15, No. 2, pp. 232-240

[11] Lieuwen, T., Torres, H., Johnson, C., and Zinn, B.T., 2001, "A Mechanism of Combustion Instability in Lean Premixed Gas Turbine Combustors," *Journal of Engineering for Gas Turbine and Power*, Vol. 123, pp. 182-188

[12] Lee, H.J., Kim, K.T., Lee, J.G., Quay, B.D., and Santavicca, D., 2009, "An Experimental Study on the Coupling of Combustion Instability Mechanisms in a Lean Premixed Gas Turbine Combustor," *Proceedings of ASME Turbo Expo 2009*, GT2009-60009

[13] Lee, J.G., Kim, K., and Santavicca, D.A., 2000, "Measurement of Equivalence Ratio Fluctuation and Its Effect on Heat Release during Unstable Combustion," *Proceedings of the Combustion Institute*, Vol. 28, The Combustion Institute, Pittsburgh, PA, pp. 415-421

[14] Waser, M.P., and Crocker, M.J., 1984, "Introduction to the Two-Microphone Cross-Spectral Method of Determining Sound Intensity," *Noise Control Engineering Journal*, April, 1984

[15] Abom, M., and Boden, H., 1988, "Error Analysis of Two-microphone Measurements in Ducts with Flow," *Journal of Acoustic Society of America*, Vol. 83, No. 6, pp. 2429-2438

[16] Lee, H.J., 2009, "Combustion Instability Mechanisms in a Lean Premixed Gas Turbine Combustor," Ph.D. dissertation, The Pennsylvania State University, University Park, PA

[17] Mongia, R.K., Tomita, E., Hsu F.K., Talbot L., and Dibble, R.W., 1996, "Use of an Optical Probe for Time-resolved In Situ Measurement of Local Air-to-Fuel Ratio and Extent of Fuel Mixing with Applications to Low NOx Emissions in Premixed Gas Turbines," *Proceedings of the Combustion Institute*, Vol. 26, The Combustion Institute, Pittsburgh, PA, pp. 2749-2755

[18]Tomita, E., Kawahara N., Yoshiyama, S., Kakuho, A., Itoh, T., and Hamamoto Y., 2002, "In Situ Fuel Concentration Measurement near Spark Plug in Spark-Ignition Engines by 3.39 μm Infrared Laser Absorption Technique," *Proceedings of the Combustion Institute*, Vol. 29, The Combustion Institute, Pittsburgh, PA, pp. 735-741

[19] Gabrielson, T., 2008, Chapter 2 in "Acoustic Data Measurements and Analysis," Lecture Notes, Graduate Program in Acoustics, The Pennsylvania State University, University Park, PA, August